STEM CELLS TRANSLATIONAL MEDICINE®

TISSUE-SPECIFIC PROGENITOR AND STEM CELLS

Transplantation of CD15-Enriched Murine Neural Stem Cells Increases Total Engraftment and Shifts Differentiation Toward the Oligodendrocyte Lineage

SUSHMA CHAUBEY,[a] JOHN H. WOLFE[a,b,c]

Key Words. Neural stem cell • Cell surface markers • Stem cell transplantation • Multipotential differentiation • Oligodendrocytes • FACS • Neural differentiation

[a]Research Institute of the Children's Hospital of Philadelphia, Philadelphia, Pennsylvania, USA; [b]W.F. Goodman Center for Comparative Medical Genetics, School of Veterinary Medicine, and [c]Department of Pediatrics, Perelman School of Medicine, University of Pennsylvania, Philadelphia, Pennsylvania, USA

Correspondence: John H. Wolfe, V.M.D., Ph.D., 502G Abramson Pediatrics Research Center, Children's Hospital of Philadelphia, Philadelphia, Pennsylvania 19104, USA. Telephone: 215-590-7028; Fax: 215-590-3779; E-Mail: jhwolfe@vet.upenn.edu

Received August 27, 2012; accepted for publication March 1, 2013; first published online in SCTM *EXPRESS* May 16, 2013.

1066-5099/2013/$20.00/0

http://dx.doi.org/10.5966/sctm.2012-0105

ABSTRACT

Neural stem cell (NSC) transplantation is a promising therapeutic approach for neurological diseases. However, only a limited number of cells can be transplanted into the brain, resulting in relatively low levels of engraftment. This study investigated the potential of using a cell surface marker to enrich a primary NSC population to increase stable engraftment in the recipient brain. NSCs were enriched from the neonatal mouse forebrain using anti-CD15 (Lewis X antigen, or SSEA-1) in a "gentle" fluorescence-activated cell sorting protocol, which yielded >98% CD15-positive cells. The CD15-positive cells differentiated into neurons, astrocytes, and oligodendrocytes in vitro, after withdrawal of growth factors, demonstrating multipotentiality. CD15-positive cells were expanded in vitro and injected bilaterally into the ventricles of neonatal mice. Cells from enriched and unenriched donor populations were found throughout the neuraxis, in both neurogenic and non-neurogenic regions. Total engraftment was similar at 7 days postinjection, but by 28 days postinjection, after brain organogenesis was complete, the survival of donor cells was significantly increased in CD15-enriched grafts over the unenriched cell grafts. The engrafted cells were heterogeneous in morphology and differentiated into all three neural lineages. Furthermore, in the CD15-enriched grafts, there was a significant shift toward differentiation into oligodendrocytes. This strategy may allow better delivery of therapeutic cells to the developing central nervous system and may be particularly useful for treating diseases involving white matter lesions. STEM CELLS TRANSLATIONAL MEDICINE *2013;2:444–454*

INTRODUCTION

Neural stem cells (NSCs) are a potential source for cell-mediated therapy in neurogenetic and neurodegenerative diseases [1–4]. Clinical trials are ongoing for the use of neural stem cells for different neurological diseases [5, 6]. The emergence of pluripotent stem cells that can differentiate into a variety of special neural phenotypes has stimulated additional trials for developing cell-based intervention of neurological diseases [7]. However, the conditions for reliable, well-tolerated, and effective cell therapies in brain disease are not yet fully established. Both preclinical data that uncover the basic biology of NSC, offering a more solid rational for the design of clinical studies, and pilot trials to ensure the safety and feasibility issues of NSC transplantation need to be addressed for a successful clinical trial.

Previous studies have shown that it is possible to deliver a therapeutic protein in the mouse brain by transplantation of immortalized NSCs [8, 9]. Cell lines have been very useful for certain experiments, but since they are immortalized clones, they do not represent the heterogeneous population of NSCs that would be used for ex vivo gene therapy with a patient's own cells. However, primary NSCs are limited in the ability to survive and migrate in vivo [10–12], necessitating strategies to improve engraftment. Transplantation for therapeutic applications in the brain is also limited by the number of cells that can be safely injected. Thus, we assessed whether enrichment for an early NSC population could increase the total amount of stable engraftment in recipient brains.

Previous studies have used fluorescence-activated cell sorting (FACS) for various markers to enrich different mouse NSC subpopulations [13–17]. We chose to enrich the CD15 population because studies suggest that it plays an important role in migration and in growth factor signaling: (a) anti-CD15 antibodies disturb migration, aggregation, adhesion, and process formation of various neural cell types, including NSCs, astrocytes, and neurons [18–20]; and (b) CD15-containing glycans can modulate growth factor

signaling and notch signaling pathways to affect proliferation and self-renewal [21–23].

We analyzed CD15-enriched and unenriched NSCs for their ability to survive, migrate, and differentiate in vivo after transplantation into neonatal mouse ventricles. NSCs were enriched for CD15-positive cells using a "gentle" FACS procedure to preserve cell viability. CD15-enriched NSCs showed more robust engraftment than unenriched NSCs at 4 weeks post-transplantation. In addition, after differentiation, the CD15-enriched NSC grafts had significantly more oligodendrocytes compared with the unenriched grafts. Better survival of donor cells, injected into the developing brain, may be useful for therapeutic delivery in diseases with dispersed lesions, and the increased differentiation into oligodendrocytes in vivo may be particularly useful for diseases affecting white matter.

Materials and Methods

Animals

C3H/SCID and transgenic green fluorescent protein (GFP) mice (C57BL/6-Tg(CAG-EGFP)131Osb/LeySopJ) were obtained from the Jackson Laboratory (Bar Harbor, ME, http://www.jax.org) and were maintained in a breeding colony at the Children's Hospital of Philadelphia. The GFP transgenic mouse line contains "enhanced" GFP cDNA under the control of a chicken β-actin promoter and cytomegalovirus enhancer. Animal procedures were performed in accordance with the NIH Guide for the Care and Use of Laboratory Animals and were approved by the Institutional Animal Care and Use Committee of the Children's Hospital of Philadelphia.

Microdissection of Mouse Brain

Postnatal day 2, neonatal GFP mice were cryoanesthetized by placing them on ice for 4 minutes. The brains were removed and placed into a phosphate-buffered saline (PBS) solution. The subventricular zone (SVZ) was microdissected by transversely sectioning precisely caudal to the olfactory bulbs and rostral to the hippocampus. The SVZ was then separated and dissected free from the adjacent brain tissue. NSC cultures were isolated as previously described [24] with the following modifications: (a) digestion of tissue in 0.25% trypsin (Worthington Biochemical, Lakewood, NJ, http://www.worthington-biochem.com) was performed, and (b) Dulbecco's Modified Eagle's Medium: Nutrient Mixture F-12 (DMEM/F12; 1:1 ratio; Gibco-BRL, Gaithersburg, MD, http://www.invitrogen.com) culture medium was used. The cells were triturated and resuspended in 10% fetal bovine serum (FBS) plating medium (as described below). The total number of viable cells was determined by hemocytometer, and cell viability was assessed using trypan blue exclusion (0.4%; Sigma-Aldrich, St. Louis, MO, http://www.sigmaaldrich.com).

Primary Murine NSC Culture

The isolated NSCs were plated into 25-cm^2 tissue culture flasks (Corning Costar, Acton, MA, http://www.corning.com/lifesciences) coated with 10 μg/ml poly-L-lysine (Sigma-Aldrich) and expanded as reported previously [24]. Briefly, the cells were plated in 10% serum-containing plating medium consisting of DMEM/F12 with supplements and growth factors. After 48 hours, the medium was changed to feeding medium consisting of DMEM/F12 supplemented with 1% N2 supplement (Gibco-BRL), 1% penicillin, streptomycin, and fungizone (PSF) solution (Gibco-BRL), 1% L-glutamine (Gibco-BRL), 1% FBS, 20 ng/ml epidermal growth factor (Promega, Madison, WI, http://www.promega.com), 20 ng/ml basic fibroblast growth factor (Promega), and 10 μg/ml heparin (Sigma-Aldrich). The NSC cultures were maintained at 37°C in humidified 5% carbon dioxide tissue culture incubators. Cultures were fed every 2–3 days by changing half of the medium and adding fresh growth factors. Cultures were passaged and subcultured every 6–8 days by gently dissociating with TrpLE Express (Invitrogen, Carlsbad, CA, http://www.invitrogen.com). TrpLE was used for dissociation of the cells in culture, which also improves viability [25]. Cell doubling time was determined as described earlier [24]. NSCs obtained after two passages were processed for fluorescence-activated cell sorting.

Fluorescence-Activated Cell Sorting

For flow cytometry, the cells were resuspended in PBS and passed through a 40-μm cell strainer (BD Biosciences, San Diego, CA, http://www.bdbiosciences.com) to separate nondissociated clumps. The GFP-positive NSCs were blocked with 5% BSA solution in PBS and divided into two samples: (a) CD15-enriched NSC sample, which was labeled for surface NSC marker CD15 and sorted for double-positive (CD15+ and GFP+) cells, and (b) unenriched NSC sample, not labeled with anti-CD15, but passed through the sorter under identical conditions and sorted for all GFP-positive cells. All of the treatments of the unenriched versus enriched samples were identical, except for the presence or absence of primary CD15 antibody. For CD15 staining, the sample was incubated with anti-CD15 monoclonal antibody (MMA clone; BD Pharmingen, San Diego, CA, http://www.bdbiosciences.com; 25 μl in 100 μl of cell suspension of 1×10^6 cells) in staining solution (3% BSA/PBS) for 20 minutes at 4°C. Unenriched NSC sample was incubated in the staining solution (3% BSA/PBS) without CD15 antibody. NSCs from both samples were washed in PBS and then were incubated in secondary fluorescent-conjugated antibody (Millipore, Billerica, MA, http://www.millipore.com; goat anti-mouse IgM Cy5, 1:300) on ice for 15 minutes. The cells were washed and resuspended in the sort buffer containing 1% BSA, 5 mM EDTA, and 1% glucose for cell sorting on FACSVantage SE with DiVa option (BD Biosciences). 4′,6-Diamidino-2-phenylindole (DAPI; Invitrogen; 1 μg/ml) was used for staining to exclude dead cells. The collected data were additionally analyzed using FlowJo software (Tree Star, Ashland, OR, http://www.treestar.com). Background fluorescence was measured using unlabeled cells and was used to set gating parameters between positive and negative cell populations. Cell aggregations and small debris were excluded from isolation on the basis of side scatter and forward scatter. Gentle FACS conditions were used (100-μm nozzle, 15 psi, 30-kHz drop-drive frequency) [26]. Postsort purity of enriched NSC population was determined. The sorted cells were replated in the NSC medium for two passages to increase the number of cells before injections into the host brains.

Immunocytofluorescence and Immunohistofluorescence

For immunocytofluorescence and immunohistofluorescence, the cells were washed with PBS and fixed for 15 minutes in 4% paraformaldehyde (PFA; Sigma-Aldrich) in PBS, pH 7.4. After another wash with PBS, the cells were incubated in blocking solution (5% normal goat serum in PBS-0.1% Triton X-100 for immunocytofluorescence and 10% normal goat serum in PBS-0.3%

Table 1. Extent of donor cell distribution along brain axes

Days post-transplant	Enrichment	Number of mice (*n*)	Rostral-caudal Mean ± SEM (mm)	Rostral-caudal Significance	Dorsal-ventral Mean ± SEM (mm)	Dorsal-ventral Significance	Medial-lateral Mean ± SEM (mm)	Medial-lateral Significance
7	None	10	6.8 ± 0.4	$p = .48$	3.1 ± 0.1	$p = .19$	3.0 ± 0.1	$p = .31$
	CD15+	12	7.2 ± 0.4		3.3 ± 0.1		3.2 ± 0.1	
28	None	8	8.3 ± 0.5	$p = .10$	3.9 ± 0.1	$p = .16$	3.1 ± 0.1	$p = .24$
	CD15+	7	9.5 ± 0.4		4.2 ± 0.1		3.4 ± 0.2	

Triton X-100 for immunohistofluorescence) for 40 minutes. The cells were incubated with the appropriate primary antibody in 3% normal goat serum in PBS-0.1% Triton X-100 solution for immunocytofluorescence and 10% normal goat serum in PBS-0.3% Triton X-100 solution for immunohistofluorescence for 60 minutes at room temperature or 4°C overnight. Following washes with PBS, the cells were incubated for 45 minutes at room temperature with the secondary antibodies, washed with PBS, and mounted in Vectashield with DAPI (Vector Laboratories, Burlingame, CA, http://www.vectorlabs.com). The cells were incubated with one of the following primary antibodies: mouse anti-nestin (1:100, Rat 401; Developmental Studies Hybridoma Bank, Iowa City, IA, http://dshb.biology.uiowa.edu/), rabbit anti-nestin (1:200; Santa Cruz Biotechnology Inc., Santa Cruz, CA, http://www.scbt.com), rabbit anti-glial fibrillary acidic protein (GFAP) (1:1,000; Millipore), anti-CD15 MMA clone (1:100; BD Pharmingen), mouse anti-tubulin, tuj1 clone (1:2,000; Millipore), rabbit anti-tubulin (1:200; Sigma-Aldrich), goat anti-doublecortin (DCX) (1:200; Santa Cruz), mouse anti-MAP2ab (1:300; Millipore), and APC/CC1 (1:100; Millipore). Appropriate fluorescent-conjugated secondary antibodies (1:250 dilution) were used including fluorescein isothiocyanate (FITC)-conjugated goat anti-rabbit IgG, FITC-conjugated goat anti-mouse IgG+M, Alexa Fluor 594 goat anti-rabbit IgG (H+L), Alexa Fluor 594 goat anti-mouse IgG (H+L), Alexa Fluor 594 donkey anti-goat IgG, or rhodamine-conjugated goat anti-mouse IgG (all from Molecular Probes, Eugene, OR, http://probes.invitrogen.com). For galactosylceramidase (GalC) immunostaining, live cells were stained with the primary GalC hybridoma antibody (1:1; kind gift from Dr. J. Grinspan, Children's Hospital of Philadelphia) and secondary antibodies (1:250; rhodamine-conjugated goat anti-mouse IgG; Molecular Probes) followed by 4% PFA fixation. The images were captured and analyzed using a fluorescence microscope (AF6000 LX; Leica, Heerbrugg, Switzerland, http://www.leica.com) and CCD camera (DFC 360FX; Leica) or confocal microscope (FV1000, Olympus, Center Valley, PA, http://www.olympusamerica.com; or LSM510 META NLO, Carl Zeiss, Jena, Germany, http://www.zeiss.com).

Cell Preparation and Transplantation

NSCs harvested from the forebrain of GFP mice were sorted and expanded in vitro for two passages. The cells were injected in a suspension of 2 μl of PBS (60,000–90,000 cells) bilaterally into the ventricles of neonatal SCID mice at postnatal day 1 or 2. There were no apparent differences in engraftment whether the cells were injected at postnatal day 1 or 2. Transplantation procedures were similar to those previously detailed [8]. On the day of transplantation, tissue culture flasks containing 80%–90% confluent cells were trypsinized, and NSCs were resuspended in sterile PBS for injection. The cells were maintained on ice during surgery, and the remaining cells were analyzed for cell viability using trypan blue dye exclusion afterward.

Tissue Processing

The animals were deeply anesthetized and transcardially perfused using normal saline followed by 4% PFA in PBS. The brains were dissected and transferred to a solution of 4% PFA overnight, washed in PBS+NaN_3, and then embedded in 2% agarose. Serial coronal vibratome-cut sections (six series, 50 μm thick) were processed for histology and immunofluorescence analysis. Sections were mounted with Vectashield mounting medium containing DAPI or were immunostained with neural lineage markers and were visualized using immunofluorescence microscope or confocal microscope. All images used for quantification were captured with identical settings.

Cell Counts and Image Acquisition

The number of engrafted cells was assessed in 50-μm-thick coronal brain sections. The cells were counted in every sixth section from each transplanted animal, resulting in 20–25 sections being analyzed per animal, which were evenly spaced throughout the rostrocaudal extent of the brain (three or four mice per treatment group). Data acquisition was performed by one person, who was blinded to the status of donor cells, and repeated three times. The triple counts yielded very low variance for all analyses, thus validating the precision of the manual counting method. The engrafted cells were counted separately for distribution, percentage survival, and differentiation. The distribution was measured as the farthest extent of GFP+ donor cells found in each of the primary brain axes (rostral-caudal, medial-lateral, and dorsal-ventral) matched to the sterotaxic brain atlas of the mouse [27], averaged for multiple animals (Table 1), and adjusted for the smaller brain dimensions of 7-day-old mice. The percentage of survival was expressed as the total number of engrafted cells counting every sixth section, divided by one-sixth of the total number of transplanted cells, multiplied by 100. Differentiation was determined by counting GFP+ cells with typical morphology for undifferentiated, neuronal, astrocytic, or oligodendrocytic cell type using fluorescent microscopy. This method of counting based on morphology was validated in representative coronal brain sections (four to six slices per group) by immunofluorescence staining with lineage-specific markers, followed by confocal microscopy analysis. The *z*-stacks were recorded on a confocal microscope using a Zeiss Plan-Neo 63×/NA 1.4 oil immersion lens with a 405-nm diode laser, 488-nm argon laser, and 568-nm krypton laser excitation wavelengths. Images were imported into ImageJ and adjusted for brightness and contrast. The correlations between morphological and immunomarker identification of cell types were determined by an exact binomial approach (R 2.15.1), which was used to construct 95% confidence intervals (CIs), which were in the range of 99%–100%, and the probability of success was in the range of 95%–100%.

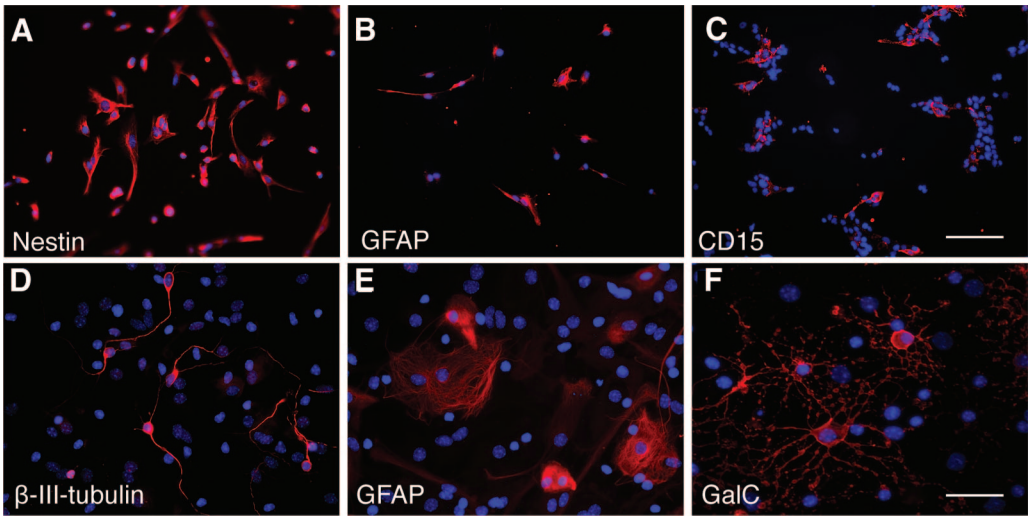

Figure 1. Neural stem cells (NSCs) isolated from forebrains of neonatal mice express NSC markers and are multipotent. **(A–C):** Immunocytochemical staining showing expression of intracellular markers nestin **(A)** and GFAP **(B)** and surface marker CD15 **(C)**. **(D–F):** Upon withdrawal of growth factors, NSCs differentiated into three neural lineages, neurons (β-III-tubulin) **(D)**, astrocytes (GFAP) **(E)**, and oligodendrocytes (GalC) **(F)**. 4′,6-Diamidino-2-phenylindole was used for counterstaining. Scale bars = 100 μm **(A–C)** and 50 μm **(D–F)**. Abbreviations: GalC, galactosylceramidase; GFAP, glial fibrillary acidic protein.

Statistical Analysis

Statistical analyses were performed using two-tailed unpaired Student's *t* test for two-group comparison with GraphPad Prizm software 5.0a for Macintosh or using one-way analysis of variance followed by Bonferroni correction. The data were log-transformed to analyze a normal distribution. Statistical significance was defined as $p < .05$. All values are expressed as means ± SEM. The number of samples per mice is indicated in the legend to each figure and in the body of the table.

Results

Neonatal SVZ NSCs Express Characteristic Stem Cell Markers and Are Multipotent

Cells isolated from neonatal GFP mouse forebrains, containing the SVZ, were grown in NSC culture conditions. After two passages, all cells expressed the NSC markers nestin and GFAP (Fig. 1A, 1B) [28–31]. CD15 was expressed in approximately 18% of the cells (Fig. 1C). NSCs were differentiated by culturing them in the absence of growth factors for 14 days. Upon withdrawal of growth factors, the cells differentiated into three neural lineages: neurons, astrocytes, and oligodendrocytes (Fig. 1D–1F), demonstrating multipotency. The NSCs proliferated in vitro with a doubling time of 5–6 days, similar to that reported earlier [24].

FACS Enrichment Yields Highly Pure Population of CD15-Positive Cells

The cells were enriched for CD15 using a gentle FACS protocol to preserve maximum viability of the cells after sorting. The cells were either sorted for GFP (the unenriched population) or for double-positive GFP/CD15 expression (the enriched population). The FACS plots for a representative preparation are shown in Figure 2. DAPI exclusion showed that approximately 76% of the cells were viable (Fig. 2A), doublets and clumps were excluded by gating (Fig. 2B, 2C), and the viable singlet cells were analyzed for GFP (Fig. 2D) or for GFP/CD15 double-positive staining (Fig. 2E). The mean for seven experiments was 97.8 ± 0.8% positive for GFP and 17.9 ± 0.6% double positive for both CD15 and GFP.

CD15+ cells directly isolated from neonatal SVZ represented 15.5 ± 1.8% of total SVZ cells (Fig. 2F), which was 4.8-fold greater than from adult brains of the same mouse strain using the same FACS conditions (3.2 ± 0.3%; data not shown). The amounts we found in the adult SVZ were similar to previous studies (3%–5%). Since the total number of CD15+ cells obtained from the neonatal brain was small, we then expanded them in NSC culture to obtain enough cells for transplantation. In culture, the percentages of CD15+ NSCs progressively increased from passage (P) 1 to P2 to P3 (7.0 ± 0.3% to 17.9 ± 0.6 to 37.8 ± 1.5%, respectively) (Fig. 2F). Postsort analysis of the CD15-enriched NSCs after P2 yielded a nearly pure population (98.2 ± 0.5%) of GFP/CD15 double-positive cells (Fig. 2F), thus sorting enriched the cells for CD15 by 5.5-fold.

Enriched and Unenriched NSCs Actively Proliferate and Show Similar Differentiation Profiles In Vitro

Samples of each preparation used for transplants were saved and analyzed for NSC markers. The CD15-enriched population was approximately 70% positive for CD15, whereas the unenriched population was approximately 20% positive (Fig. 3A–3C). Almost all NSCs were positive for both nestin (Fig. 3D–3F) and GFAP (Fig. 3G–3I) [28–31]. Some spontaneous differentiation was seen, but the amounts were not significantly different between the enriched and unenriched preparations. Both cultures were ~99% positive for the proliferative marker Ki67 (data not shown). Thus, the only significant difference in marker expression at the time of transplantation was for CD15, which was approximately 3.5 times more in the enriched population.

Transplanted CD15-Enriched and Unenriched NSCs Migrate Along the Entire Rostral-Caudal Extent of the Brain and Have Similar Patterns of Distribution Within the Recipient Brain

The enriched and unenriched NSCs were transplanted into neonatal mice by infusion into the lateral ventricles. The extent of

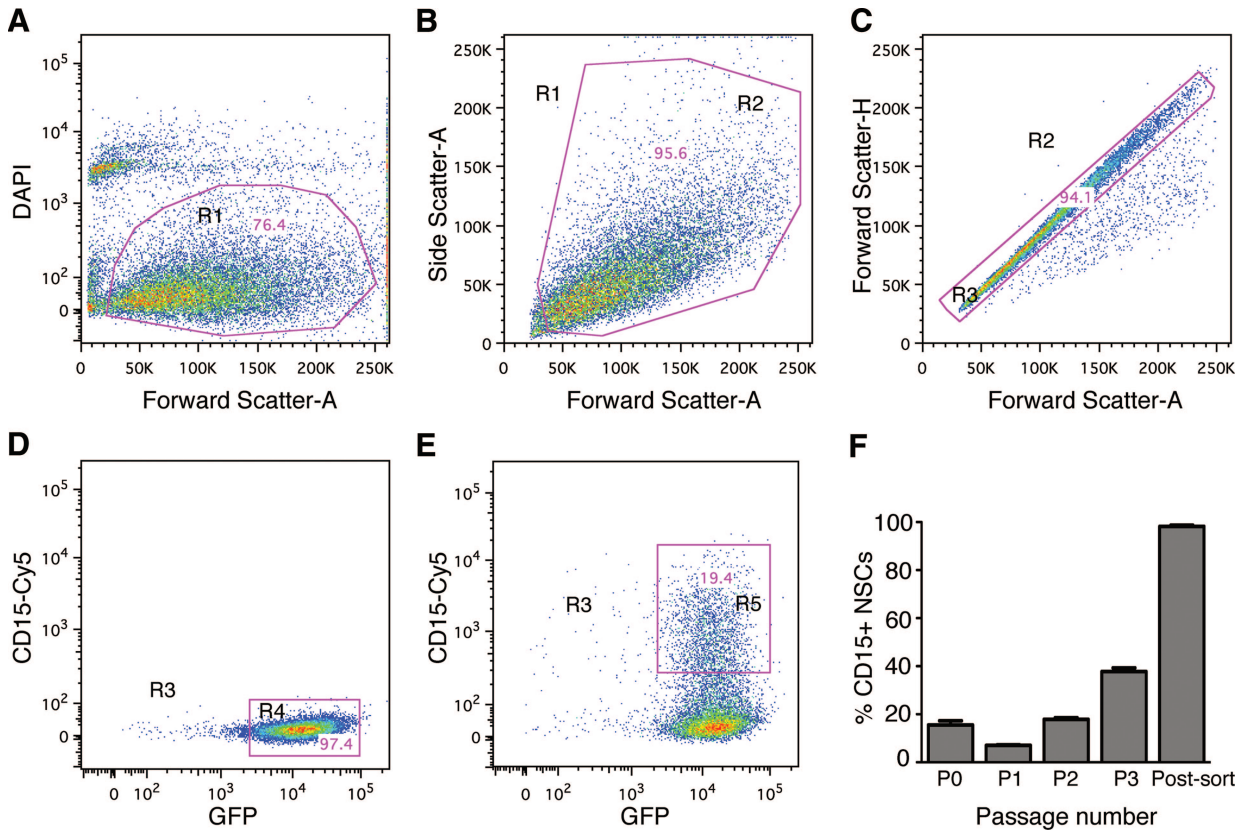

Figure 2. Fluorescence-activated cell sorting (FACS) of neural stem cells (NSCs), grown for two passages in vitro, yields a highly enriched population of CD15-positive cells. **(A–E):** Representative FACS plots showing the gating strategy for GFP+ cells. The NSC population was gated for viable cells as shown in the two-dimensional dot plot, forward scatter (FSC) versus DAPI. **(A):** Dead and damaged cells were excluded based on DAPI uptake to identify the viable cell population, R1. **(B, C):** Gated R1 viable cells were plotted based on FSC versus side scatter, R2 **(B)**, and FSC-A versus FSC-H, R3 **(C)**, to exclude doublets and clumps. **(D, E):** The gated R3 cells were plotted based on GFP and CD15-Cy5 fluorescence, and gates were drawn to define all GFP+ cells, R4 in the unenriched NSC sample **(D)**, and CD15+ GFP+ double-positive cell population in the enriched NSC population, R5 **(E)**. **(F):** Percentages of CD15+ cells isolated directly from the neonatal subventricular zone (passage [P] 0), after passages in culture (P1, P2, and P3), and postsort purity of enriched NSCs after passage 2. Purity of the postsort enriched double-positive population was >98.0%. Abbreviations: DAPI, 4′,6-diamidino-2-phenylindole; GFP, green fluorescent protein; NSC, neural stem cell; R, region.

distribution of the engrafted cells was analyzed in the rostral-caudal, dorsal-ventral, and medial-lateral axes for the unenriched and CD15-enriched grafts at 7 and 28 days postinjection (dpi). A total of 37 mice were analyzed for the extent of distribution along the axes: 22 mice at 7 dpi and 15 mice at 28 dpi. There was no significant difference ($p > .05$) between the extent of distribution of unenriched and enriched grafts both 7 and 28 dpi (Table 1). Additional mice analyzed at intermediate time points (14 and 21 dpi) showed similar distribution as seen at 7 and 28 dpi (data not shown).

A group of representative mice was analyzed for quantitative distribution of engrafted cells in different brain subregions along the rostral-caudal axis at 7 and 28 dpi. The brain was divided along the rostral-caudal axis into subregions from +6 to +2, +2 to −2, and −2 to −6 (from the bregma). Representative samples were analyzed quantitatively by counting every sixth section; however, the intermediate sections were similar in donor cell distribution. The percentage of GFP+ cells detected in the subregion to the total engrafted cells in the brain was calculated. The engrafted cells were distributed along the full extent of the rostrocaudal axis of the brain at 7 dpi (Fig. 4A) and 28 dpi (Fig. 4B). There was no significant difference between the unenriched and CD15-enriched distribution at 7 dpi ($p > .05$); however, at 28 dpi, a greater percentage of engrafted cells was detected in the subregion +6 to +2 in the unenriched recipients compared with the enriched recipients ($p < .05$).

The distribution pattern of enriched versus unenriched cells, with respect to the structures in which engrafted cells were found, was very similar at both time points ($p > .05$ for all structures). At 7 dpi, most of the donor cells were seen near the ventricles, including the aqueduct and the lateral and third ventricles. At this time point, donor cells were also seen in the olfactory bulbs, lateral septum, corpus callosum, and hypothalamus, but very few cells were present in the cerebral cortex. At 28 dpi, donor cells were found in the same structures as at 7 dpi, but also in the optic chiasm, fimbria, and amygdala. Only a few cells were detected in the thalamus, striatum, or cerebellum, and none were detected in the cerebral cortex.

CD15 Enrichment Results in Increased Survival in the Adult Brain

The percentage survival of the transplanted NSCs was determined by counting the number of GFP-positive cells in the brain at 7, 14, and 28 dpi relative to the input dose. At 7 dpi, there was no significant difference between the number of unenriched (5.1 ± 1.7%) and CD15-enriched (4.8 ± 0.2%) engrafted cells. At

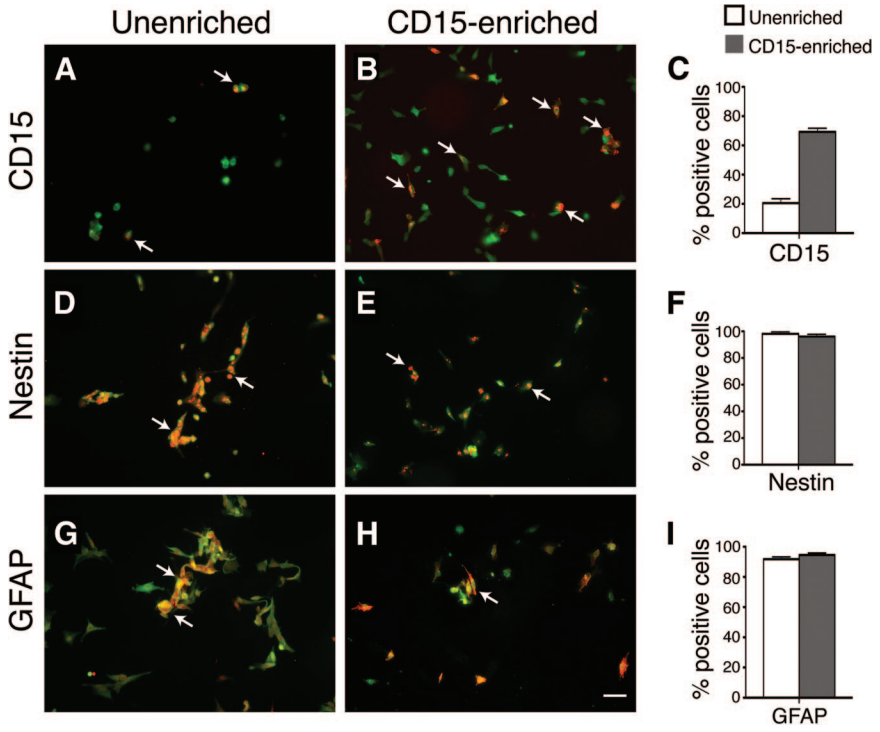

Figure 3. In vitro characterization of unenriched and enriched neural stem cells (NSCs) prior to injection show similar amounts of nestin+ and GFAP+ progenitor cells with 3.5-fold more CD15+ cells in enriched population. **(A–C):** Immunocytochemical staining for CD15 shows an increase of CD15-positive cells from 20% in unenriched NSCs to 70% in enriched NSCs. **(D–I):** Immunocytochemical staining reveals similar distribution of undifferentiated NSC markers, nestin **(D–F)** and GFAP **(G–I)**, between unenriched and enriched cells. 4′,6-Diamidino-2-phenylindole was used for counterstaining the individual cells. The histograms **(C, F, I)** represent mean percentages ± SEM of immunopositive cells from five or more representative regions. Scale bar = 50 μm in all photomicrographs. Abbreviation: GFAP, glial fibrillary acidic protein.

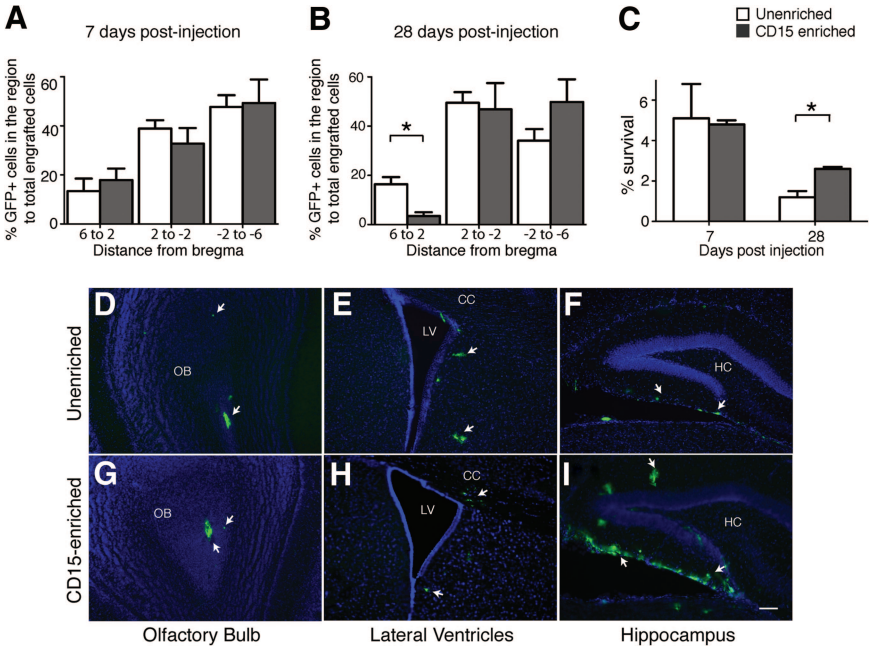

Figure 4. Unenriched and enriched neural stem cells (NSCs) migrate along the entire rostral-caudal extent of the brain and have differential survival 4 weeks post-transplantation. **(A, B):** Distribution of unenriched (white bars) versus enriched (gray bars) NSCs at specific distances from the bregma at 7 days **(A)** and 28 days **(B)** postinjection. The *x*-axis shows distance in mm; bregma is at 0 mm. The *y*-axis shows the percentage of green fluorescent protein-positive (GFP+) cells in a subregion to total engrafted cells in the brain. Percentages are the means ± SEM; $n = 3$ animals for each group. The percentage distribution of enriched versus unenriched was not significantly different at any distance at 7 days postinjection (dpi) ($p > .05$); however, at 28 dpi, the percentage distribution of the GFP+ unenriched grafts was significantly more in the 6 to 2 mm subregion as compared with the enriched NSCs. *, $p < .05$, Student's *t* test with Bonferroni correction. **(C):** Total survival of donor cells at 7 and 28 dpi. Enriched grafts were significantly increased at 28 dpi. *, $p < .05$, Student's *t* test with Bonferroni correction; $n = 3–4$ animals. **(D–I):** Representative sections show engraftment of unenriched **(D–F)** or enriched **(G–I)** at 28 dpi, from selected regions. White arrows point toward the GFP+ engrafted cells. Scale bar = 100 μm **(D–I)**. Abbreviations: CC, corpus callosum; HC, hippocampus; LV, lateral ventricle; OB, olfactory bulb.

14 dpi, the total number of cells decreased compared with the number at 7 dpi, and there also was no difference between the brains receiving enriched versus unenriched NSCs (2.4 ± 1.2% and 2.5 ± 1.0%, respectively; data not shown). In contrast, at 28 dpi the number of CD15-enriched NSCs (2.6 ± 0.1%) was significantly greater than in the unenriched grafts (1.2 ± 0.3%) ($p < .05$). No Ki67 staining was detected at 28 days in the enriched or unenriched grafts (data not shown), indicating that the donor

cells had withdrawn from mitosis. The overall increase in number of enriched NSCs was not due to significantly a larger number in any particular brain structure but rather due to a global increase across structures (Fig. 4D–4I). Overall, the CD15 enrichment led to significantly better survival in the mature brain.

Engrafted NSCs Differentiate Into All Three Neural Lineages, and CD15 Enrichment Increases Oligodendrocytes

The engrafted cells, identified by GFP, displayed the characteristic morphologies of neurons, astrocytes, and oligodendrocytes (Fig. 5A–5C). As a practical matter, in order to quantify each type of cell throughout each of the transplanted brains, it was necessary to score them by morphology. We therefore validated this approach by probing representative sections with lineage-specific immunofluorescent antibody staining for characteristic markers (Fig. 5D–5W), which correlated with the morphological identification. We used an exact binomial approach (R 2.15.1) to construct 95% CIs on the probability that a transplanted cell with particular cell morphology, as seen by the GFP signal, expressed corresponding specific cell lineage marker, as shown by the immunostaining in Figure 5. 95% CI analysis for the morphology of different cell type and their corresponding cell-lineage markers was in the range of 99%–100%, and the probability of success was in the range of 95%–100%. At 28 dpi, the immature neuronal marker DCX and the mature neuronal marker MAP2ab stained neuronal processes (Fig. 5G, 5K), anti-GFAP stained the processes of astrocytes (Fig. 5O), and APC stained the cell bodies of mature oligodendrocytes (Fig. 5S). Identification of undifferentiated NSCs was done on the basis of nestin staining. Nestin-positive undifferentiated NSCs were located adjacent to ventricles (Fig. 5W).

The percentage of cells at 7 dpi that were nestin-positive (undifferentiated), neurons, astrocytes, and oligodendrocytes was not significantly different between unenriched and enriched (undifferentiated, unenriched 35.8 $\pm$ 4.7% and enriched 33.8 $\pm$ 4.7%; neurons, unenriched 52.2 $\pm$ 6.4% and enriched 48.8 $\pm$ 10.1%; astrocytes, unenriched 11.9 $\pm$ 6.7% and enriched 16.9 $\pm$ 5.7%; oligodendrocytes, unenriched 0.2 $\pm$ 0.1% and enriched 0.5 $\pm$ 0.4%; $p > .05$) (Fig. 6). In contrast, at 28 dpi, the percentage of oligodendrocytes in the enriched grafts was significantly greater than in the unenriched grafts (unenriched 10.6 $\pm$ 0.9% and enriched 18.5 $\pm$ 0.8%; $p < .001$) (Fig. 6D), whereas the undifferentiated cells, neurons, and astrocytes were not (undifferentiated, unenriched 8.5 $\pm$ 6.9% and enriched 14.8 $\pm$ 4.9%; neurons, unenriched 44.0 $\pm$ 5.7% and enriched 31.0 $\pm$ 1.5%; astrocytes, unenriched 36.9 $\pm$ 3.4% and enriched 35.7 $\pm$ 3.1%; $p > .05$). Although the total number of enriched versus unenriched cells was not significantly different at 7 dpi, there were significantly more cells in the enriched grafts in the white matter areas of corpus callosum (678 $\pm$ 60 versus 270 $\pm$ 78, $n = 3$, $p < .05$) and external capsule (1,602 $\pm$ 72 vs. 906 $\pm$ 186, $n = 3$, $p < .05$). This suggests that in the early post-transplant period, the enriched donor population contained more progenitor cells with a tropism for developing myelinating structures, which was later reflected as an increase in oligodendrocytes in the mature grafts of CD15-enriched cells.

Discussion

The CD15 moiety is involved in modulating cell migration, adhesion, and process formation [18–20], as well as growth factor signaling involved in maintenance and differentiation [21–23, 32, 33]. CD15-containing glycans are expressed prominently in neurogenic brain regions throughout development [34]. Thus, we hypothesized that enriching NSCs for the CD15+ subpopulation would potentially be a useful step to increase survival in the transplant setting. This study demonstrates that enrichment of NSCs using the CD15 leads not only to increased survival of the transplanted NSCs but also to preferential differentiation into oligodendrocytes.

CD15 enrichment of adult SVZ cells yields a highly proliferative population of NSCs, which exhibit self-renewal and multipotency [13, 31]. In the neonatal mouse, we found approximately four times more CD15+ cells than in the adult brain (15.5% vs. 3.2%). This probably reflects the active brain remodeling and development that occur in the perinatal period, with an increasing fraction of progenitors leaving the cell cycle to become postmitotic as they mature.

FACS sorting for CD15 from the neonatal mouse forebrain yielded >98% pure CD15+ fractions, resulting in an ~6.5-fold enrichment over direct isolation from the SVZ. However, since the total number of CD15+ NSCs that could be isolated directly from the brain was limited, it was necessary to expand them in NSC culture to obtain enough cells for transplantation experiments. Since the FACS procedure is stressful for cells, we performed the enrichment using the gentle FACS [26] first and then seeded them into NSC culture medium to stabilize and expand before transplantation. The number of CD15+ cells initially decreased in the unenriched cultures but then after two passages rose to ~18%; thus, these transplants contained approximately the same proportion of CD15+ cells as they would have using the direct isolation from the SVZ. The cultures of the FACS-sorted CD15+ cells declined to ~70% during the two passages in culture, resulting in a 3.5-fold total difference in actual CD15+ cells injected in the unenriched versus enriched transplants. The CD15-depleted population was not used for transplants because CD15-negative SVZ cells have very limited self-renewal [13].

Neonatal intraventricular injections were performed in order to introduce the donor NSCs at a developmentally active phase in host brain development, when the cues for migration and maturation are present in the microenvironment [8, 35, 36]. The ventricular system provides a relatively large volume, which allows injection of a larger number of cells than intraparenchymal transplants [10, 37]. At 7 dpi, many of the donor cells were still in a progenitor stage, but they were already distributed widely. The pattern of distribution with respect to the substructures of the brain was similar to transplants of neurosphere cells [12]. At 28 dpi, donor cells were present in additional structures, and they were found farther away from the ventricles than at 7 dpi, indicating that they continued to migrate deeper into the parenchyma after the initial dispersal in the first 7 days.

The number of cells stabilized in the CD15-enriched grafts between 14 and 28 dpi (data not shown), whereas the unenriched grafts continued to decline. The improved survival was accounted for by the increase in the oligodendroglial cell lineages. This correlated with the presence of more donor cells in white matter tracts at the early time point after engraftment (7 dpi). Thus, the greater number of donor cells in the CD15-enriched grafts could be due either to better survival of the NSCs or

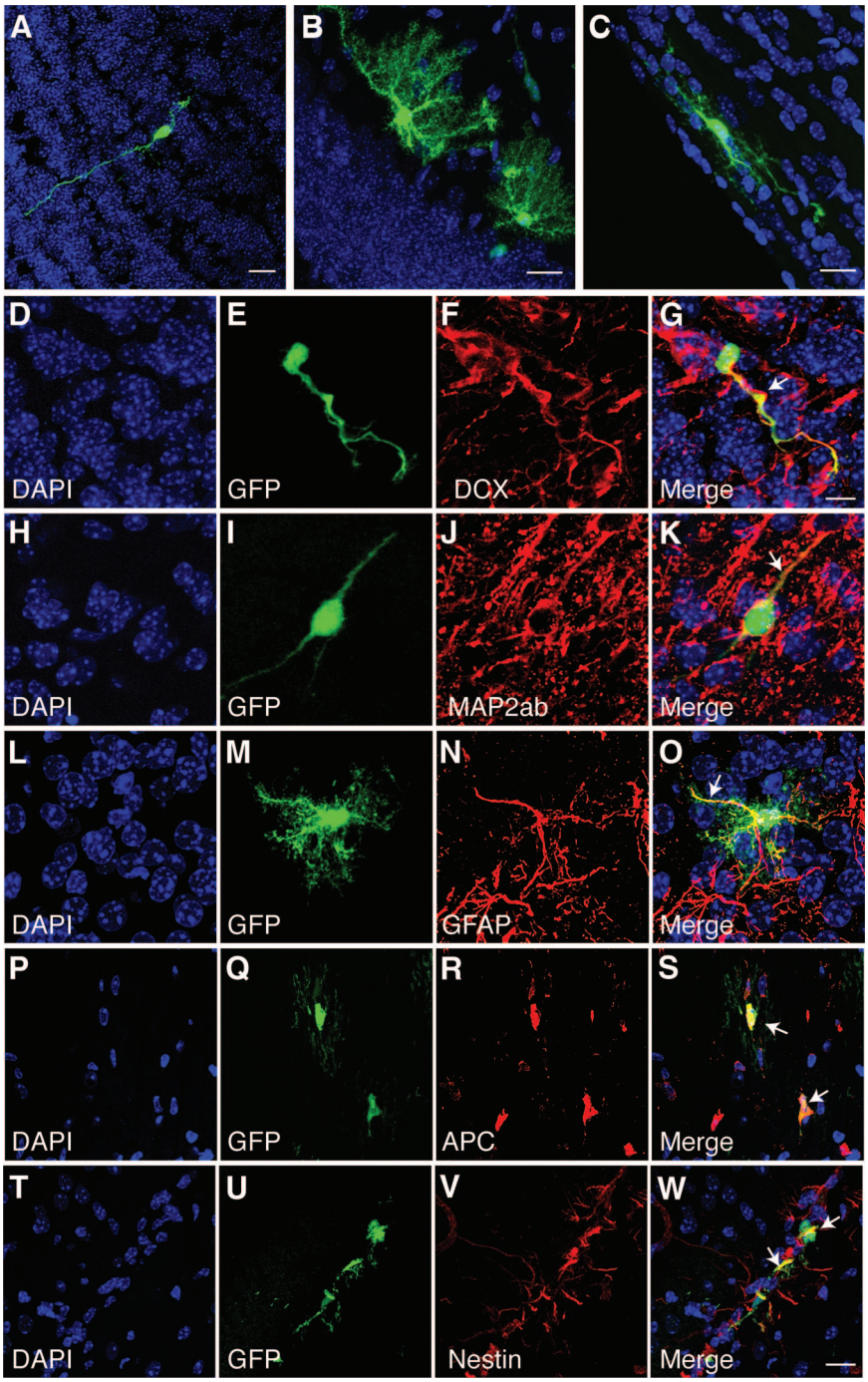

Figure 5. Engrafted neural stem cells (NSCs) show heterogeneous morphology and differentiate into different neural lineages in vivo at 28 postinjection (dpi). **(A–C):** Confocal images of engrafted cells showing typical morphology of three neural lineages, neurons **(A)**, astrocytes **(B)**, and oligodendrocytes **(C)**. **(D–W):** In vivo staining with markers for the different cell types: neurons (DCX, **D–G**; MAP2ab, **H–K**), astrocytes (GFAP, **L–O**), and oligodendrocytes (APC, **P–S**), show characteristic staining patterns. The lineage markers stained cells with corresponding morphology. **(T–W):** Undifferentiated nestin-positive NSCs were present. White arrows in the merge panels indicate cells that coexpressed GFP (green) and the lineage marker (red) in yellow. Scale bars = 20 μm **(A–C)**, 10 μm **(D–G)**, and 20 μm **(H–W)**. Abbreviations: DAPI, 4′,6-diamidino-2-phenylindole; DCX, doublecortin; GFAP, glial fibrillary acidic protein; GFP, green fluorescent protein; MAP2ab, microtubule-associated protein 2a,b.

to an expansion of the oligodendroglial progenitor cells in this fraction. By 28 dpi, there was very little staining with the proliferation marker Ki67, indicating that any expansion occurred prior to brain maturation.

The oligodendrocyte increase over time, both unenriched and enriched NSC grafts, was coincident with the postnatal development of white matter in the brain. The increase in oligodendrocytes may be mediated either by extrinsic cues present in the white matter microenvironment, to which the uncommitted transplanted cells respond and differentiate, or by intrinsic properties of lineage-restricted oligodendroglial progenitors selected by the enrichment for CD15. In support of the former, the CXCR4 chemokine receptor is coexpressed with CD15 in mouse SVZ cells [38] and plays an important role in increasing survival and migration

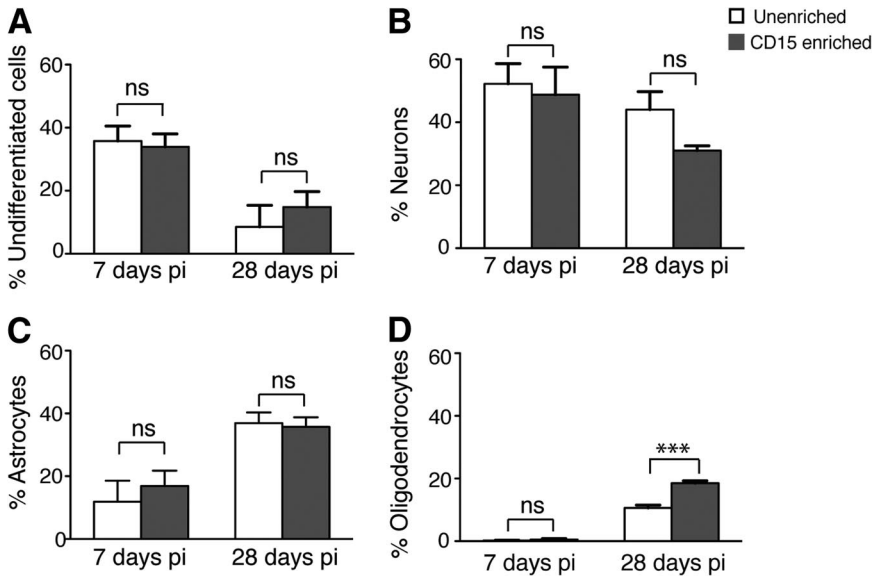

Figure 6. CD15 enrichment leads to increased oligodendrocyte differentiation at 28 days postinjection (dpi). **(A–D):** Histograms demonstrating populations of green fluorescent protein-positive and nestin-positive undifferentiated neural stem cells (NSCs) **(A)**, doublecortin-positive and microtubule-associated protein 2a,b-positive neurons **(B)**, glial fibrillary acidic protein-positive astrocytes **(C)**, and APC+ oligodendrocytes **(D)** at 7 and 28 days post-transplantation. The *x*-axis depicts unenriched and CD15-enriched populations at 7 and 28 dpi, and the *y*-axis shows the percentage of different phenotypes in total engrafted cells in the brain. **(A):** The percentage of nestin-positive cells (undifferentiated NSCs) does not show any significant difference between unenriched and enriched grafts, either at 7 dpi (ns, $p > .05$) or 28 dpi (ns, $p > .05$). **(B):** The percentage of neurons does not show any significant difference between unenriched and enriched grafts both 7 and 28 dpi (ns, $p > .05$). **(C):** The percentage of astrocytes does not show any significant difference at 7 and 28 dpi between unenriched (ns, $p > .05$) and enriched (ns, $p > .05$). **(D):** A significant increase in percentage of oligodendrocytes was seen in enriched NSC grafts compared with the unenriched grafts at 28 dpi. ***, $p < .001$. The percentages are the means ± SEM; $n = 3$ animals for each group, one-way analysis of variance with Bonferroni correction, $p < .05$. Abbreviations: ns, not significant; pi, postinjection.

of oligodendrocyte precursors into the corpus callosum [39–41]. In addition, SDF-1, a ligand of CXCR4, is expressed in the corpus callosum, and the CXCR4-SDF pathway has been shown to enhance CD15-CXCR4 chemotaxis, proliferation, and survival [38].

Labeling mitotic cells in the SVZ of the adult mouse brain has shown that type B1 NSCs, which coexpress GFAP, CD15, and nestin [42], migrate to white matter tracks and differentiate into oligodendrocytes [43, 44]. Thus, the CD15-enriched NSCs in our study appear to be type B1 cells because they were also positive for GFAP and nestin. In our experiments, CD15 enrichment increased the number of donor cells located in white matter structures, such as the corpus callosum and external capsule, at the earlier time point (7 dpi) after transplantation. This suggests that soon after transplantation, the enriched donor population contained more progenitor cells with a tropism for developing myelinating structures, resulting in more oligodendrocytes in the mature grafts of CD15-enriched cells. Accordingly, the transplanted cells in our experiments appear to integrate into the same migratory routes as those used by endogenous progenitors that populate white matter tracts [43, 45].

CD15 expression closely parallels that of another NSC surface marker, CD133 (Prominin-1), in mouse brain cells and has been suggested to identify similar cell types [25]. These antigens are useful for characterizing similar subpopulations from the human central nervous system [46, 47], which is sustained in the expanded neurosphere cells, and also mark subfractions of neurosphere-initiating cells [48]. This similarity between CD15 and CD133 (Prominin-1) extends the application of this study to larger animal models.

To our knowledge, this is the first quantitative assessment of CD15-enriched primary NSCs in vivo in terms of survival, distribution, and differentiation within the brain of a postnatal mouse. The increased survival of CD15-enriched cells may be useful for therapeutic delivery in diseases with dispersed lesions. The increased differentiation into oligodendrocytes in vivo may be useful for treating diseases affecting white matter that can be addressed by neonatal delivery of NSCs.

Conclusion

Primary SVZ NSCs from neonatal mice that were FACS-enriched for surface marker CD15 and transplanted into neonatal recipients were distributed along the neuraxis at early and late time points after injection. CD15 enrichment resulted in significantly greater donor cell survival than with unenriched NSCs. In vivo, the engrafted cells of either type could differentiate into all three neural lineages (neurons, astrocytes, and oligodendrocytes), but a significant increase in oligodendrocytic differentiation occurred after CD15 enrichment. Thus, CD15 enrichment of NSCs may improve the therapeutic potential of NSC transplantation, particularly for treating diseases involving white matter lesions.

Acknowledgments

We thank T. Clark and A. Polesky for expert technical assistance, the Wolfe laboratory members for excellent discussions, H. Pletcher and the Penn Flow Cytometry and Cell Sorting Facility for advice and assistance, the Penn Cell and Developmental Biology Microscopy Core for confocal imaging, and Dr. M. Putt from the Biostatistics and Epidemiology Core for consultation with the statistics (Intellectual and Developmental Disabilities

Research Center Grant P30-HD026979). This work was supported by Grant R01-NS056243 from the National Institute of Neurological Disorders and Stroke, NIH.

Author Contributions

S.C.: conception and design, collection and assembly of data, data analysis and interpretation, manuscript writing, final approval of manuscript; J.H.W.: conception and design, financial support, collection and/or assembly of data, data analysis and interpretation, manuscript writing, final approval of manuscript.

Disclosure of Potential Conflicts of Interest

The authors indicate no potential conflicts of interest.

References

1 Snyder EY, Wolfe JH. Central nervous system cell transplantation: A novel therapy for storage diseases? Curr Opin Neurol 1996;9:126–136.

2 Shihabuddin LS, Palmer TD, Gage FH. The search for neural progenitor cells: Prospects for the therapy of neurodegenerative disease. Mol Med Today 1999;5:474–480.

3 Lindvall O, Kokaia Z. Stem cells for the treatment of neurological disorders. Nature 2006;441:1094–1096.

4 Martino G, Pluchino S. The therapeutic potential of neural stem cells. Nat Rev Neurosci 2006;7:395–406.

5 Trounson A, Thakar RG, Lomax G et al. Clinical trials for stem cell therapies. BMC Med 2011;9:52.

6 Chiu AY, Rao MS. Cell based therapy for neural disorders-anticipating challenges. Neurotherapeutics 2011;8:744–752.

7 Gupta N, Henry RG, Strober J et al. Neural stem cell engraftment and myelination in the human brain. Sci Transl Med 2012;4:155ra137.

8 Snyder EY, Taylor RM, Wolfe JH. Neural progenitor cell engraftment corrects lysosomal storage throughout the MPS VII mouse brain. Nature 1995;374:367–370.

9 Flax JD, Aurora S, Yang C et al. Engraftable human neural stem cells respond to developmental cues, replace neurons, and express foreign genes. Nat Biotechnol 1998;16:1033–1039.

10 Shihabuddin LS, Numan S, Huff MR et al. Intracerebral transplantation of adult mouse neural progenitor cells into the Niemann-Pick-A mouse leads to a marked decrease in lysosomal storage pathology. J Neurosci 2004;24:10642–10651.

11 Magnitsky S, Walton RM, Wolfe JH et al. Magnetic resonance imaging detects differences in migration between primary and immortalized neural stem cells. Acad Radiol 2008;15:1269–1281.

12 Neri M, Ricca A, di Girolamo I et al. Neural stem cell gene therapy ameliorates pathology and function in a mouse model of globoid cell leukodystrophy. Stem Cells 2011;29:1559–1571.

13 Capela A, Temple S. LeX/ssea-1 is expressed by adult mouse CNS stem cells, identifying them as nonependymal. Neuron 2002;35:865–875.

14 Barraud P, Thompson L, Kirik D et al. Isolation and characterization of neural precursor cells from the Sox1-GFP reporter mouse. Eur J Neurosci 2005;22:1555–1569.

15 Corti S, Nizzardo M, Nardini M et al. Isolation and characterization of murine neural stem/progenitor cells based on Prominin-1 expression. Exp Neurol 2007;205:547–562.

16 Hamanoue M, Matsuzaki Y, Sato K et al. Cell surface N-glycans mediated isolation of mouse neural stem cells. J Neurochem 2009;110:1575–1584.

17 Nakatani Y, Yanagisawa M, Suzuki Y et al. Characterization of GD3 ganglioside as a novel biomarker of mouse neural stem cells. Glycobiology 2010;20:78–86.

18 Yanagisawa M, Taga T, Nakamura K et al. Characterization of glycoconjugate antigens in mouse embryonic neural precursor cells. J Neurochem 2005;95:1311–1320.

19 Streit A, Nolte C, Rasony T et al. Interaction of astrochondrin with extracellular matrix components and its involvement in astrocyte process formation and cerebellar granule cell migration. J Cell Biol 1993;120:799–814.

20 Lieberoth A, Splittstoesser F, Katagihallimath N et al. Lewis(x) and alpha2,3-sialyl glycans and their receptors TAG-1, contactin, and L1 mediate CD24-dependent neurite outgrowth. J Neurosci 2009;29:6677–6690.

21 Capela A, Temple S. LeX is expressed by principle progenitor cells in the embryonic nervous system, is secreted into their environment and binds Wnt-1. Dev Biol 2006;291:300–313.

22 Koso H, Ouchi Y, Tabata Y et al. SSEA-1 marks regionally restricted immature subpopulations of embryonic retinal progenitor cells that are regulated by the Wnt signaling pathway. Dev Biol 2006;292:265–276.

23 Yagi H, Saito T, Yanagisawa M et al. Lewis X-carrying *N*-glycans regulate the proliferation of mouse embryonic neural stem cells via the notch signaling pathway. J Biol Chem 2012;287:24356–24364.

24 Heuer GG, Skorupa AF, Prasad Alur RK et al. Accumulation of abnormal amounts of glycosaminoglycans in murine mucopolysaccharidosis type VII neural progenitor cells does not alter the growth rate or efficiency of differentiation into neurons. Mol Cell Neurosci 2001;17:167–178.

25 Panchision DM, Chen HL, Pistollato F et al. Optimized flow cytometric analysis of central nervous system tissue reveals novel functional relationships among cells expressing CD133, CD15, and CD24. Stem Cells 2007;25:1560–1570.

26 Pruszak J, Sonntag KC, Aung MH et al. Markers and methods for cell sorting of human embryonic stem cell-derived neural cell populations. Stem Cells 2007;25:2257–2268.

27 Paxinos G, Franklin KBJ. The mouse brain in stereotaxic coordinates. San Diego, CA: Academic Press, 1997.

28 Mignone JL, Kukekov V, Chiang AS et al. Neural stem and progenitor cells in nestin-GFP transgenic mice. J Comp Neurol 2004;469:311–324.

29 Doetsch F, Caille I, Lim DA et al. Subventricular zone astrocytes are neural stem cells in the adult mammalian brain. Cell 1999;97:703–716.

30 Imura T, Kornblum HI, Sofroniew MV. The predominant neural stem cell isolated from postnatal and adult forebrain but not early embryonic forebrain expresses GFAP. J Neurosci 2003;23:2824–2832.

31 Imura T, Nakano I, Kornblum HI et al. Phenotypic and functional heterogeneity of GFAP-expressing cells in vitro: Differential expression of LeX/CD15 by GFAP-expressing multipotent neural stem cells and non-neurogenic astrocytes. Glia 2006;53:277–293.

32 Dvorak P, Hampl A, Jirmanova L et al. Embryoglycan ectodomains regulate biological activities of FGF-2 to embryonic stem cells. J Cell Sci 1998;111:2945–2952.

33 Jirmanova L, Pacholikova J, Krejci P et al. O-linked carbohydrates are required for FGF-2 mediated proliferation of mouse embryonic cells. Int J Dev Biol 1999;43:555–562.

34 Hennen E, Czopka T, Faissner A. Structurally distinct LewisX glycans distinguish subpopulations of neural stem/progenitor cells. J Biol Chem 2011;286:16321–16331.

35 Lee JP, McKercher S, Muller FJ et al. Neural stem cell transplantation in mouse brain. Curr Protoc Neurosci 2008;42:3.10.1–3.10.23.

36 Rao MS, Vemuri MC. Neural transplantation and stem cells. Methods Mol Biol 2009;549:3–16.

37 Watson DJ, Walton RM, Magnitsky SG et al. Structure-specific patterns of neural stem cell engraftment after transplantation in the adult mouse brain. Hum Gene Ther 2006;17:693–704.

38 Corti S, Locatelli F, Papadimitriou D et al. Multipotentiality, homing properties, and pyramidal neurogenesis of CNS-derived LeX(ssea-1)+/CXCR4+ stem cells. FASEB J 2005;19:1860–1862.

39 Tran PB, Banisadr G, Ren D et al. Chemokine receptor expression by neural progenitor cells in neurogenic regions of mouse brain. J Comp Neurol 2007;500:1007–1033.

40 Dziembowska M, Tham TN, Lau P et al. A role for CXCR4 signaling in survival and migration of neural and oligodendrocyte precursors. Glia 2005;50:258–269.

41 Banisadr G, Frederick TJ, Freitag C et al. The role of CXCR4 signaling in the migration of transplanted oligodendrocyte progenitors into the cerebral white matter. Neurobiol Dis 2011;44:19–27.

42 Ihrie RA, Alvarez-Buylla A. Lake-front property: A unique germinal niche by the lateral ventricles of the adult brain. Neuron 2011;70:674–686.

43 Menn B, Garcia-Verdugo JM, Yaschine C et al. Origin of oligodendrocytes in the subventricular zone of the adult brain. J Neurosci 2006;26:7907–7918.

44 Gonzalez-Perez O, Romero-Rodriguez R, Soriano-Navarro M et al. Epidermal growth factor induces the progeny of subventricular zone type B cells to migrate and differentiate into oligodendrocytes. Stem Cells 2009;27:2032–2043.

45 Parent JM, von dem Bussche N, Lowenstein DH. Prolonged seizures recruit caudal subventricular zone glial progenitors into the injured hippocampus. Hippocampus 2006;16:321–328.

46 Uchida N, Buck DW, He D et al. Direct isolation of human central nervous system stem cells. Proc Natl Acad Sci USA 2000;97:14720–14725.

47 Peh GS, Lang RJ, Pera MF et al. CD133 expression by neural progenitors derived from human embryonic stem cells and its use for their prospective isolation. Stem Cells Dev 2009;18:269–282.

48 Barraud P, Stott S, Mollgard K et al. In vitro characterization of a human neural progenitor cell coexpressing SSEA4 and CD133. J Neurosci Res 2007;85:250–259.